Fabrication of Carbon Nanotube Field Emission Tip Array Based on Laser Processing and Research on the Characteristics of Field Emission Array

Wei-Che Lin[1], Kao-Jen Lin[1] and Hung-Yin Tsai[1,#]

1 Department of Power Mechanical Engineering, National Tsing Hua University, Hsinchu, Taiwan
Corresponding Author / Email: hytsai@pme.nthu.edu.tw , TEL: +886-03-5742343

KEYWORDS: Carbon nanotube, Field emission, Laser processing, Tip array, Chemical vapor deposition

The floating catalyst chemical vapor method was used to deposit carbon nanotube films, and the catalyst is ferrocene powder. At constant gas volume flow and reaction gas temperature, the height of carbon nanotubes can be changed by controlling the growth time. The proposed carbon nanotube films have good alignment and conductivity and are very suitable for use as a field emission cathode. Then, laser processing was used to fabricate the carbon nanotube needle tip array to improve field emission properties. We first studied the minimum time required to produce a carbon nanotube film that completely covers the substrate and its corresponding height of carbon nanotubes. After producing a uniform film, we fabricate carbon nanotubes with different laser spacing parameters. For the carbon nanotube tip array, the effects of the laser spacing and carbon nanotube height on the field emission characteristics were discussed.

1. Introduction

1.1. Carbon Nanotubes

Carbon nanotubes (CNTs) were accidentally discovered by Iijima Sumio in 1991 using a transmission electron microscope [1]. They are needle-like structures generated by graphite cathodes during arc discharge. They possess good electrical conductivity, thermal stability, and collimation, making them ideal for field emission cathode applications. The general growth method involves depositing the catalyst metal on the substrate through sputtering or evaporation, followed by growth in a high-temperature furnace tube. However, this exposes the catalyst to air, causing oxidation and deactivation of the catalyst during growth. To address this issue, Kinoshita et al. [2] proposed a two-step process. In the floating catalyst chemical vapor deposition method, the ferrocene catalyst/ethanol mist is first deposited on the substrate after thermal oxidation using an ultrasonic atomizer. Then, a carbon source is introduced for growth. By keeping the catalyst all in the cavity, this method avoids oxidation and preserves catalyst activity.

1.2. Heat Affect Zone in Laser Processing

The heat affected zone is due to the accumulation of high energy density near the surface of the material, which increases the temperature of the material. When metal materials undergo thermal cycling and the temperature reaches their melting point, the material will sublime as the temperature keeps rising. As can be seen in Fig. 1, in the case of laser drilling, spatter, oxide, and recast layer formation, a heat-affected zone will occur during processing, and the heat-affected zone can be adjusted by adjusting the processing parameters or laser wavelength to achieve an increase in quality after processing.

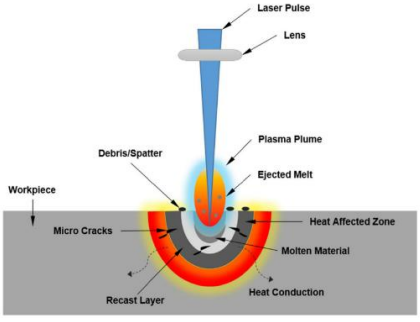

Fig. 1 Schematic illustration of physical damage that occurs during nanosecond/millisecond laser drilling [3]

1.3. Field Emission Effect

Under normal conditions, due to the absence of external energy, the electrons are hard to escape from the material body due to the potential barrier on the material surface. To make electrons leave the

material surface, it needs to apply energy to the material in three ways: photoelectron emission, thermionic emission, and field emission. Photoelectron emission means that the energy on the surface of the material is greater than its work function so that the electrons gain energy and then leave the surface of the material [6,7], as shown in Fig. 2. Also, surface topography will affect the field emission characteristics [8-15].

The growth method used in CNT in this study is the floating catalyst chemical vapor deposition method. Then, the carbon nanotubes will be laser-cut to produce needle-shaped field emission arrays and then measured by field emission. In this research, the effect of the obtained carbon nanotube topography on the field emission characteristics will be compared under different spacing and heights.

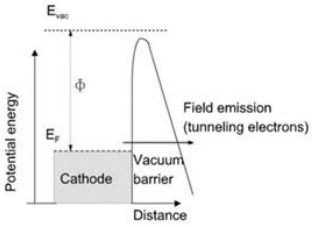

Fig. 2 Band structure of vacuum barrier bending during field emission [6]

2. Experiment Method

2.1 Preparation of Lasered CNT Array

This research used a high-temperature furnace tube, as shown in Fig. 3, to produce carbon nanotubes by a floating catalyst chemical vapor method. Ferrocene powder was placed on the catalyst carrier 15 cm from the substrate. Inert gases He and Ar were used as carrier gases, and C_2H_2 was used as a carbon source gas. The detailed experiment condition of CNT growth can be seen in Fig. 4.

THE M320F-UDT900M laser engraver was used to cut the thin film into carbon nanotube arrays by laser. The frequency was set to 20 kHz, and the scanning speed was fixed to 5 mm/s. The array was lasered according to different spacings. Experiments with the same spacing were used to measure the effect of CNT height on field emission characteristics.

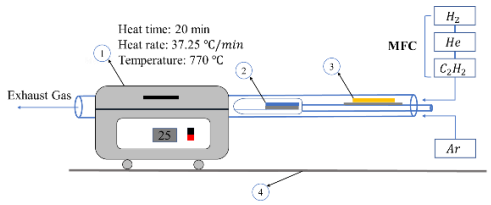

Fig. 3 Floating catalyst chemical vapor deposition method. (1) High-temperature furnace tube, (2) quartz carrier, (3) catalyst carrier, and (4) furnace tube slide

2.2 Characteristics of Lasered CNT

The morphologies of lasered CNT will be scanned and recorded by SEM (TM-3030 Plus). The field emission characteristics of the lasered CNT are measured in a vacuum condition, and the voltage is applied from 0 V to 600 V.

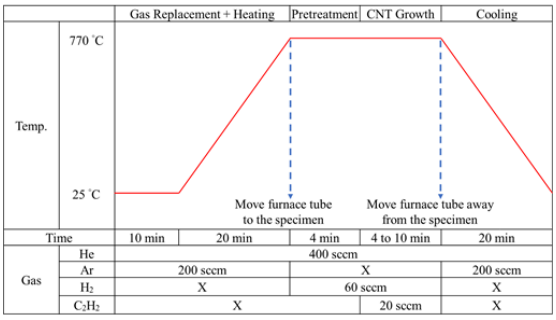

Fig. 4 The process parameters of CNT growth of temperature, time, and inert gas in each stage

3. Result and Discussion

3.1 Relationship between CNT Height and Growth Time

In Fig. 5, it can be found that the growth height and coverage area of carbon nanotubes increases with the increase of time. The height is uneven at 4 minutes; the average height at 6 and 15 minutes are 135 and 300 μm, respectively. It is worth mentioning that the coverage of carbon nanotubes is very different at 4 minutes and 6 minutes. At 6 minutes, carbon nanotubes almost cover the entire substrate, and the growth density and quality are higher than at 4 minutes.

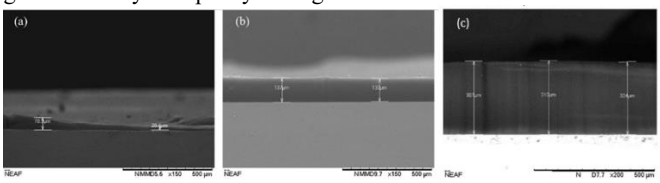

Fig. 5 SEM side view of CNT growth time at (a) 4 min, (b) 6 min, and (c) 15 min

3.2 Optimization of Laser Spacing

A laser with a frequency of 20 kHz, a scanning speed of 5 mm/s, and a laser power of 1 W were selected for cutting carbon nanotube tip arrays. The actual laser kerf width was 85 μm. Therefore, the laser spacing was designed to be 75 μm and 100 μm to get the needle tip and trapezoid shape. The reason for choosing 75 μm is to explore the impact of overlap area on the morphology and field emission properties of carbon nanotubes.

Fig. 6(a) shows the un-lasered carbon nanotube film with a uniform and flat morphology, 300 μm in height. In Fig. 6(b), with a laser spacing of 75 μm, the carbon nanotube height decreases, and the needle tips become irregularly arranged, leading to the loss of some whisker tips during field emission. Fig. 6(c), with a laser spacing of 100 μm, depicts a neat and needle-like laser array without overlapping, suitable for field emission with a 15 μm tip size.

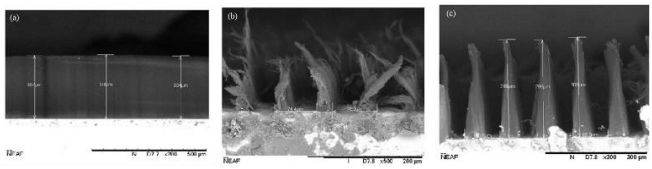

Fig. 6 SEM side view of (a) CNT film without laser processing and with laser processing of CNT array with different laser spacing of (b) 75 μm and (c) 100 μm

Then, field emission of different laser spacings and pristine carbon nanotube films will be compared, as shown in Fig. 7 and Table 1. In J-E plot, the further left of the curve, the lower energy required for field emission. In Table 1, laser spacing of 100μm shows the most optimized performance with the smallest turn-on and threshold field. Laser spacing of 75 μm had the irregular whisker-shaped carbon nanotubes, this may burn or destroy during the field emission process, which leads to a higher threshold field.

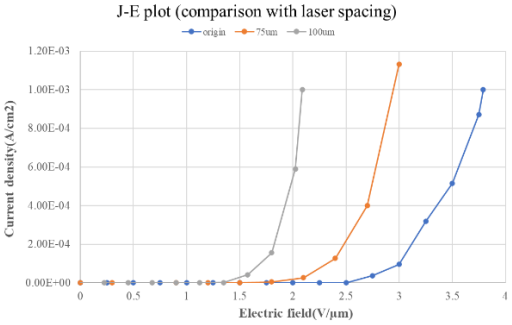

Fig. 7 Comparison of CNT arrays J-E plots with different laser spacings

Table 1 Turn-on field and threshold field at each laser distance

	Turn-on field (V/μm)	Threshold field (V/μm)
Origin	2.563	3.792
75 μm	1.861	2.946
100 μm	1.398	2.088

3.3 Optimization of CNT Array Tip Width

After the deciding laser spacing, a shorter tip size, 5 μm, was chosen to avoid trapezoid-like shapes. Fig. 8 shows the side view of the CNT tip array in 15 and 5 μm tip widths. It can be predicted that a smaller tip width will lead to improved turn-on and threshold fields due to the enhancement of local electric fields. This will make it easier for electrons to overcome resistance and escape from the tip.

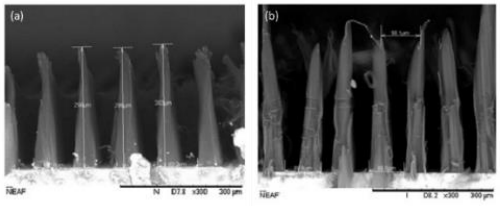

Fig. 8 Side view of the CNT tip array after laser processing. (a) T15_D100, (b) T5_D100

3.4 Optimization of CNT Array Tip Height

Heights of 150 μm was added for comparison with the previously studied height of 300 μm, and their SEM side view is shown in Fig. 9. Adjustments were made to the laser array drawing to achieve a 5 μm needle tip width by narrowing the distance between the lasers for lower heights. Higher heights may result in better field emission performance due to larger array volumes providing sufficient electrons for emission.

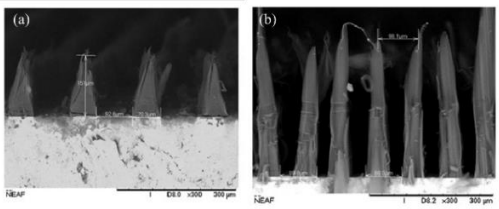

Fig. 9 Side view of different heights of CNT tip array after laser processing of sample (a) T5_D100_H150 and (b) T5_D100_H300

4. Conclusions

The field emission characteristics under different morphology of lasered CNT arrays were discussed in this research. For laser spacing larger than the laser kerf width, the larger the spacing, the more the tip topography resembled a trapezoid, leading to worse turn-on fields. For laser spacing smaller than the laser kerf width, an irregular whisker-shaped CNT appeared for the spacing. Also, some predictions were made. First, the smaller the tip width, the better the turn-on field. Second, the higher the tip of the CNT, the more the tip volume can be increased, providing enough electrons to pass through. By optimizing the parameters of the carbon nanotube tip array, an improved field emission properties will be achieved.

ACKNOWLEDGEMENT

The authors greatly appreciate the support of the National Science and Technology Council, Taiwan, under the project number 111- 2221-E-007-067-MY3.

REFERENCES

1. Iijima, S., "Helical microtubules of graphitic carbon," Nature, vol. 354, p. 56, 1991.
2. Kinoshita, T., Karita, M., Nakano, T., Inoue, Y., "Two step floating catalyst chemical vapor deposition including in situ fabrication of catalyst nanoparticles and carbon nanotube forest growth with low impurity level," Carbon, vol. 144, pp. 152-160, 2019.
3. Iralal Morar, N., Roy, R., Mehnen, J., Marithumu, S., Gray, S., Roberts, T., Nicholls, J., "Investigation of recast and crack formation in laser trepanning drilling of CMSX-4 angled holes," The International Journal of Advanced Manufacturing Technology, vol. 95, pp. 4059-4070, 2018.
4. Singh, R., J. Alberts, M., Melkote, S. N., "Characterization and prediction of the heat-affected zone in a laser-assisted mechanical micromachining process," International Journal of Machine Tools and Manufacture, vol. 48, pp. 994-1004, 2008.
5. Gbordzoe, S., Yarmolenko, S., Kanakaraj, S., Haase, M. R., Alvarez, N. T., Borgemenke, R., i Adusei, P. K., Shanov, V., " Effects of laser cutting on the structural and mechanical properties of carbon nanotube assemblages," Materials Science and

Engineering B, vol. 223, pp. 143-152, 2017.

6. Yilmazoglu, O., Evtukh, A., Al-Daffaie, S., Biethan, J.P., Pavlidis, D., Litovchenko, V., Hartnagel, H.L., "Electron field emission from nanostructured semiconductors under photo illumination," Turkish Journal of Physics, vol. 38, pp. 543-562, 2014.
7. Li, Y., Sun, Y. and Yeow, J., "Nanotube field electron emission: principles, development, and applications," Nanotechnology, vol. 26, p. 242001, 2015.
8. He, J., Cutler, P., and Miskovsky, N., "Generalization of Fowler–Nordheim field emission theory for nonplanar metal emitters," Applied Physics Letters, vol. 59, no. 13, pp. 1644-1646, 1991.
9. Jensen, K. and Zaidman, E., "Field emission from an elliptical boss: Exact versus approximate treatments," Applied Physics Letters, vol. 63, no. 5, pp. 702-704, 1993.
10. Jensen, K. and Zaidman, E., "Field emission from an elliptical boss: Exact and approximate forms for area factors and currents," Journal of Vacuum Science & Technology B: Microelectronics and Nanometer Structures Processing, Measurement, and Phenomena, vol. 12, no. 2, pp. 776-780, 1994.
11. Jensen, K. and Zaidman, E., "Analytic expressions for emission characteristics as a function of experimental parameters in sharp field emitter devices," Journal of Vacuum Science & Technology B: Microelectronics and Nanometer Structures Processing, Measurement, and Phenomena, vol. 13, no. 2, pp. 511-515, 1995.
12. Ławrowski, R., Langer, C., Prommesberger, C., Dams, F., Bachmann, M., and Schreiner, R., "Fabrication and simulation of silicon structures with high aspect ratio for field emission devices," in 2014 27th International Vacuum Nanoelectronics Conference (IVNC). IEEE, pp. 193-194, 2014.
13. Hung-Yin Tsai and Po-Tang Tseng, “Field emission characteristics of diamond nano-tip array fabricated by anodic aluminum oxide template with nano-conical holes,” Applied Surface Science, Vol. 351, pp. 1004-1010, 2015
14. Hung-Yin Tsai and Ping-Huan Tsai, “Fabrication and Field Emission Characteristic of Microcrystalline Diamond/Carbon Nanotube Double-layered Pyramid Arrays,” Thin Solid Films, Vol. 584, pp. 330-335, 2015
15. Tsai, H. Y. and Yeh, C. C., “Suppressed screening effects in curvilinear tetrahedral diamond field emitter arrays fabricated on anodic aluminum oxide,” Journal of the Electrochemical Society, Vol. 159, No. 1, pp. K1-K4, 2012